



An experimental investigation of metamorphism induced microstructure evolution in a model cohesive snow

by Michael Quast Edens

A thesis submitted in partial fulfillment of the requirements for the degree of Doctor of Philosophy In Engineering Applied Mechanics Option

Montana State University

© Copyright by Michael Quast Edens (1997)

Abstract:

Data describing snow microstructure is needed in order to verify theoretical models and the results obtained from numerical simulation of related processes. Unfortunately, such data is almost non-existent. One area of snow science where this deficiency is having an impact is in studies of microstructure metamorphism. Typically theoretical metamorphism models treat snow as an aggregate of spherical ice-grains. Adequate data describing spherical ice-grain metamorphism is non-existent. The lack of data primarily stems from the fact that the observation and measurement of microstructure is accomplished via surface sections. The location and identity of several of the most important features must be deduced from the cross sectional information that is present in order to make appropriate measurements. In the past, doing this in a consistent and objective manner has not been very successful.

The problem of consistency and objectivity has been solved by automating the feature identification and measurement process. To do this a set of criteria have been developed which characterize the microstructure appearing on a surface section. These provide a consistent and objective method for locating bond and neck cross sections. In addition a new relation has been developed which provides a way of measuring average neck length.

To begin providing some of the microstructure data needed for metamorphism studies, an experimental investigation of microstructure induced microstructure evolution has been performed. Four sets of 12 spherical ice-grain compacts were allowed to undergo microstructure induced metamorphism at one of four temperatures (-2°C, -5°C, -10°C, -15°C) for a period of five weeks. At various intervals surface sections were prepared from these samples which were then photographed using a CCD camera. Microstructure analysis was conducted using a computer program which incorporates the automated identification and measurement processes just mentioned. Results presented include bond, neck, and grain growth over time.

An extensive set of new data, detailing microstructure evolution in spherical ice-grain compacts, is now available. It was obtained using automated identification and measurement procedures. The major problems regarding identification and measurement consistency and objectivity have been solved.

AN EXPERIMENTAL INVESTIGATION OF METAMORPHISM INDUCED
MICROSTRUCTURE EVOLUTION IN A "MODEL" COHESIVE SNOW

by

Michael Quast Edens

A thesis submitted in partial fulfillment
of the requirements for the degree

of

Doctor of Philosophy

In

Engineering

Applied Mechanics Option

MONTANA STATE UNIVERSITY-BOZEMAN
Bozeman, Montana

May 1997

D378
Ed28

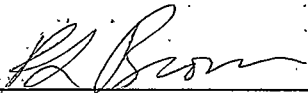
APPROVAL

of a thesis submitted by

Michael Quast Edens

This thesis has been read by each member of the thesis committee and has been found to be satisfactory regarding content, English usage, format, citations, bibliographic style, and consistency, and is ready for submission to the College of Graduate Studies.

Robert L. Brown



(Signature)

6/12/97
Date

Approved for the Department of Mechanical Engineering

Vic Cundy



(Signature)

5/16/97
Date

Approved for the College of Graduate Studies

Robert L. Brown



(Signature)

6/12/97
Date

STATEMENT OF PERMISSION TO USE

In presenting this thesis in partial fulfillment of the requirements for a doctoral degree at Montana State University-Bozeman, I agree that the Library shall make it available to borrowers under rules of the Library. I further agree that copying of this thesis is allowable only for scholarly purposes, consistent with "fair use" as prescribed in the U.S. Copyright Law. Request for extensive copying or reproduction of this thesis should be referred to University Microfilms International, 300 North Zeeb Road, Ann Arbor, Michigan 48106, to whom I have granted "the exclusive right to reproduce and distribute my dissertation in and from microform along with the non-exclusive right to reproduce and distribute my abstract in any format in whole or in part".

Signature



Date

6/13/97

TABLE OF CONTENTS

LIST OF TABLES	vi
LIST OF FIGURES	vii
ABSTRACT	x
1. SNOW	1
1.1 Introduction	1
1.2 Snow Microstructure and Microstructure Metamorphism	4
The Role of Surface Area in Microstructure Metamorphism	5
Temperature Gradient Metamorphism	6
Sintering and Geometry Driven Metamorphism	7
1.3 Measurement of Snow Microstructure	11
1.4 The Current State of Snow Mechanics and Snow Physics	14
1.5 Purpose of this Work	14
2. STEREOLOGY	16
2.1 Terminology, Concepts, and Basic Measurement	17
Basic Statistical Relationships	17
Microstructure and Phases	20
Image Sampling	24
2.2 Stereology Formulae	25
Volume Fraction	25
Surface Area to Volume Ratio	26
Mean Intercept Length	29
2.3 Volume Weighted Mean Particle Volume	31
2.4 Circular Disks	35
2.5 Edge Effects and Guard-Zones	37
3. DIGITAL SKELETONIZATION	41
3.1 Definition of the Skeleton	43
3.2 Digital Neighborhoods and Connectivity	44
3.3 Skeletonization	45

	The Distance Map	46
	Crest Points	48
	Connection Points	50
	Thinning and Partial Pruning	50
3.4	A Pictorial Example	52
4.	MODELING AND MEASUREMENT OF BONDS AND NECKS	57
4.1	Grain, Bond, and Neck Components of Consolidated Snow	59
4.2	Profiles and Skeletons	62
	Skeletons and Profile Shape	62
	Skeletons and Boundary Curvature	64
	Identification Criteria	69
4.3	Stereology of Bonds and Necks	74
	Neck Frustum	75
	Stereology of a Right Circular Cone Frustum	77
5.	MICROSTRUCTURE EVOLUTION	83
5.1	Experiment	83
5.2	Surface Section Analysis Results	87
5.3	Sensitivity of Measured Values to Bond Constriction Ratio	104
6.	CONCLUSIONS	107
	Recommendations	108
	REFERENCES CITED	110

LIST OF TABLES

Table	Page
1. Pixel resolution, magnifications, and image areas for each temperature/time series. Only the first hour of a series which has the indicated statistics is listed.....	86
2. Area fractions and specific surface areas. These are measured prior to bond segmentation of an image.	89
3. Mean grain intercept length and mean spherical grain radius. The spherical grain radius is based upon the diameters corresponding to maximal inscribed skeleton disks for each identified grain.	93
4. The first and second moments of the volume weighted mean grain volume.....	96
5. Bond radius and bond area.....	98
6. Mean neck half length.....	103

LIST OF FIGURES

Figure	Page
1. An example of probe measurements. 9 test points in the reference space (intersections of vertical and horizontal lines) intersect the gray-phase 3 times to give a point fraction $P_P(\text{gray}) = 3/9$. Three test lines, each of length L , intercept the gray-phase boundary, black curves, 12 times to give $I_L(\text{black}) = 12/3L$ for the number of point profiles per unit length of test line. There are 6 grey-phase linear profiles from the three line probes, giving $N_L(\text{gray}) = 6/3L = 2/L$ as the number of linear profiles per unit prove length. Within the dashed area A there are 5 grey-phase area profiles, which gives $N_A(\text{gray}) = 5/A$ for the number or area profiles per unit area.....	23
2. A point sampled particle and intercepts generated by a random test line through the test point.	33
3. This shows the relationships between a randomly oriented disk of radius R_i , which has been intersected by a sectioning plane. The intersection of the plane and the disk is a straight line of length $d_i = 1/m_i$	37
4. Example of a surface section A_S , view frame or quadrat A_q , and a guard-zone A_{gz} . A_{gz} is the largest rectangular region that does not intersect any object not wholly contained within A_q . For each object in the figure, there is only a single associated point (black dots) per object. Only those objects which have an associated point lying within an associated point analysis area A_{ap} are considered in any associated analysis. In the figure $A_{ap} = A_{gz}$	38
5. The disk centered at y is a maximal disk in X . The disk centered at u is not a maximal disk in X since it can be contained in larger disks also in X	44
6. Neighborhood of a point u for a digital domain. Possible paths between neighbors shown by the solid lines.	45
7. The set X is transformed by equations (25) and (26) into the distance map shown on the right. Points not in X all have distance values of zero.....	48
8. Each neighborhood shown without a central value was formed using the coding scheme described in the text. (a) Assignment of 1 to the central point creates a neighborhood satisfying criteria 1. (b) Assignment of the value 0 to the central point	

creates a neighborhood satisfying criteria 2. 1 could be assigned and then criteria 3 would be satisfied. (c) By assigning 1 to the central point criteria 3 is satisfied. A 0 could be assigned so that criteria 2 is satisfied. Notice in (b) for example that the two neighbors with values of 0 are not connected unless 0 is assigned to the central point.	49
9. A skeleton end point configuration. 1 is the end point. 1 and 2 correspond to points in $\Sigma_A(X)$	52
10. Part of a surface section.	53
11. The binary representation of Figure 10.....	53
12. The distance map corresponding to grains (black) of Figure 11.	54
13. The crest points corresponding to the distance map of Figure 12. Note how disconnected these are.	55
14. The connected skeletons for the grains of Figure 11. Each skeleton is the union of a set of crest points, illustrated in Figure 13, and the additional set of points needed to connect that skeleton's crest points.....	55
15. A thinned and partially pruned version of the skeletons shown in Figure 14.....	56
16. Part of an ice network showing grains, bonds, and necks.	60
17. Grains g_1 and g_2 along with neck η_p connecting them.	61
18. A cross section through a bonded grain pair showing the boundary profile and bond line location.	63
19. Geometry of boundary and skeleton.	65
20. An ice profile partitioned into grain, neck, and bond profiles.....	70
21. Profile of a bonded grain pair showing the bond line d_b and two neck base lines d_{η_1}, d_{η_2} . Also illustrated is the correspondence between two tangents $\hat{t}_{S1}, \hat{t}_{S2}$, at each s of S_B and the respective boundary tangents, $\hat{t}_{B1}, \hat{t}_{B2}$. Note: $\hat{t}_{S2} = -\hat{t}_{S1}$ and where corresponding skeleton and boundary tangents are required to satisfy $\hat{t}_S \circ \hat{t}_B \geq 0$	74
22. Right cone frustum.....	76
23. Top view of a frustum cross section. Necked regions generally have a concave profile rather than the convex shape shown.	81

24. A portion of a surface section in binary form. Ice profiles are shown in black. The white is pore filler.	88
25. Ratio of ice surface area to sample volume, $S_V(t)$, as a function of time. Error bars indicate standard error of the mean.....	90
26. Mean pore intercept length λ_π , as function of time.	91
27. The image of Figure 24 with the skeleton overlaid.	92
28. Mean 3-D particle intercept length, L_{3g} , as function of time. Standard mean error bars shown.	94
29. Mean radius of the maximum radius spheres inscribable in the ice grains.	95
30. Mean particle volume weighted volume, \bar{v}_V . Standard mean error bars shown.	95
31. The log of the normalized standard deviation of the volume weighted mean volume as a function of the log of the normalized volume weighted mean volume.	97
32. Specific surface area of ice, $S_{V_i}(t)$, vs. volume weighted mean grain volume, v_V	97
33. Mean 3-D bond radius, R_b , as function of time. Standard mean error bars are shown.....	99
34. Mean bond area, A_b , as function of time. Standard mean error bars are shown..	99
35. Mean number of bonds per unit surface area of grain N_{3S} , as a function of time.	100
36. Average bond radius R_b vs. average grain radius R_g	101
37. Shown is Figure 27 after neck identification and segmentation.	102
38. Mean 3-D neck length, H_η , as a function of time. Standard mean error bars are shown.....	103
39. Mean neck half length H_η vs. mean grain specific surface area $S_V(g)$	104
40. Dependence of size measurements on choice of the critical constriction ratio. .	105
41. Dependence of count based measurement upon the choice of the critical constriction ratio.	106

ABSTRACT

Data describing snow microstructure is needed in order to verify theoretical models and the results obtained from numerical simulation of related processes. Unfortunately, such data is almost non-existent. One area of snow science where this deficiency is having an impact is in studies of microstructure metamorphism. Typically theoretical metamorphism models treat snow as an aggregate of spherical ice-grains. Adequate data describing spherical ice-grain metamorphism is non-existent. The lack of data primarily stems from the fact that the observation and measurement of microstructure is accomplished via surface sections. The location and identity of several of the most important features must be deduced from the cross sectional information that is present in order to make appropriate measurements. In the past, doing this in a consistent and objective manner has not been very successful.

The problem of consistency and objectivity has been solved by automating the feature identification and measurement process. To do this a set of criteria have been developed which characterize the microstructure appearing on a surface section. These provide a consistent and objective method for locating bond and neck cross sections. In addition a new relation has been developed which provides a way of measuring average neck length.

To begin providing some of the microstructure data needed for metamorphism studies, an experimental investigation of microstructure induced microstructure evolution has been performed. Four sets of 12 spherical ice-grain compacts were allowed to undergo microstructure induced metamorphism at one of four temperatures (-2°C , -5°C , -10°C , -15°C) for a period of five weeks. At various intervals surface sections were prepared from these samples which were then photographed using a CCD camera. Microstructure analysis was conducted using a computer program which incorporates the automated identification and measurement processes just mentioned. Results presented include bond, neck, and grain growth over time.

An extensive set of new data, detailing microstructure evolution in spherical ice-grain compacts, is now available. It was obtained using automated identification and measurement procedures. The major problems regarding identification and measurement consistency and objectivity have been solved.

CHAPTER 1

SNOW

1.1 Introduction

Seasonal snow is an essential part of our natural environment. Often we don't appreciate the impact it has on our lives. It can be a source of recreation and at the same time become a deadly avalanche. In many parts of the world, the water stored in snow packs is the primary source of water during the summer and autumn. Snow can have a large influence on the net exchange of solar radiation with the earth.

In the form of avalanches, snow may be responsible for millions of dollars lost each year, due to road closures, property damage, and destroyed forest land in the U.S. and Canada alone. Construction of highway avalanche sheds, diversions, dikes and barriers on avalanche paths above highways, villages and resorts are also extremely expensive as defensive measures. In terms of human costs, hundreds of lives are lost each year, with many more than that who are fortunate enough to be rescued alive.

These are some of the reasons that prediction and control of avalanches are important aspects of snow research. Knowledge of avalanche formation, snow strength, and those changes that may actually decrease their danger are some of the things needed for accurate prediction. Avalanche control, which may occur in the form of intentional initiation of ava-

lanches with the use of explosives and projectiles, or in the form of flow control through barriers, dikes, and diversions, requires knowledge of wave propagation in snow, factors influencing that, and the stresses produced by avalanches when impacting structures.

Snow also plays a crucial role in providing a continuous source of fresh water during spring and summer months. It accounts for over 1/3 of the water used world wide for irrigation (Stepphun 1981). Being able to predict the water runoff from mountain snow packs is important for effective regulation of dams and potential floods. Typically snow hydrologist want to know such things as time of melt, quantity and rate of water released, volume of water entering soil, and amount of evaporation. This requires a knowledge of how volumetric decrease in snow water equivalent is governed by such factors as snow melt, evaporation, condensation, and transmission of water to the soil (Male 1981).

Earth's climate is also influenced by snow through its emissivity, reflection, and the absorption of solar radiation (e.g. Berry 1981; Warren 1982; Dozier et al. 1987). A related area, which is of interest to the military, is radar interaction with snow cover (Mellor 1977).

Even though snow is a granular material, its behavior, properties and processes, often fall far outside those normally encountered in traditional studies of granular materials. One very unique property of snow is its high compressibility (Mellor 1977). Relative displacements in excess of 99% possible (Yosida 1963). Much of the temperature range of interest in snow studies, finds snow near its melting temperatures. As a result of its high compressibility and elevated temperatures, we are dealing with a highly non-linear, highly temperature dependent, granular material. The factor underlying all of this is snow's highly variable microstructure. Snow's mechanical (e.g. Yosida 1963; Hobbs 1965; Keeler

1969; Kry 1975a,b; Gubler 1978a,b; Brown 1979a,b; Hansen and Brown 1986,1987; Edens and Brown 1991, Brown and Edens 1991), thermodynamic (e.g. Kingery 1960; Yosida 1963; Hobbs and Mason 1964; Colbeck 1980, 1983,1993; Adams and Brown 1990; Adams and Sato 1993; Brown et al. 1994,1996,1997a,b), and electromagnetic (e.g. Warren 1982) properties and associated processes are all direct outcomes of its microstructure. Measurement of the material microstructure has long been a central goal of past research efforts (e.g. Yosida 1963; Hobbs and Mason 1964; Colbeck 1980; Brown et al. 1994,1996,1997a,b).

Considering the importance of microstructure, it would seem that significant progress in its characterization and measurement would have occurred. Yet, as should become clear by the end of this chapter, there is a definite lack of relevant microstructure measurements and still considerable work to be done in characterization. Much of this lack is due to difficulties inherent in characterizing and measuring snow's microstructure. In this thesis, it will be demonstrated that most of the factors which have hampered progress in microstructure measurement can be overcome. As will be shown in Chapter 4, microstructural characterizations, required for the measurement process, can be stated as a set of well defined criteria. They are stated in terms of an image transformation technique (skeletonization), reviewed in Chapter 3, which also provides the framework around which automation of the entire measurement process can be based (Chapter 3 and 4). Automation is accomplished in the form of computer software. That is demonstrated in Chapter 5 where it is used to analyze microstructural evolution of aggregates of spherical ice particles. The measurements presented in that chapter are based upon the material of Chapter 2.

The experimental portion of this thesis (Chapter 5) is concerned with microstructure metamorphism. The general importance of metamorphism and its influence on snow science as a whole was noted by Colbeck in a session summary from the 1995 workshop "Future Directions in Snow and Ice Research" (Brown and Dent: editors, 1995). The first part of this chapter looks at several aspects of metamorphism of dry snow microstructure. Issues regarding characterization of snow microstructure and its measurement are then presented in section 1.3. Finally, in section 1.4 the purpose of this thesis will be stated.

1.2 Snow Microstructure and Microstructure Metamorphism

Structurally, snow is a granular material. It may be either consolidated or loose. Consolidated (cohesive) snow is characterized by a continuous ice network, formed through cohesion between ice grains, to form a porous structure. One feature of this microstructure is that over a wide density range it is a relatively open self-supporting structure. It could be described as being akin to a tinker toy structure where the grains coincide with the tinker toy joint blocks and the interconnecting structure coincides with the connecting sticks. This is contrasted to most other granular materials which are more akin to what would be obtained by dumping tinker toy joints into a pile. Typically cohesive forms of seasonal snow have densities $0.05 \text{ g/cm}^3 \leq \rho \leq 0.65 \text{ g/cm}^3$. Porosities (pore volume fraction) may vary from as low as 0.20 to as large as 0.95. A loose or weakly bonded form of snow, depth hoar, is normally found with densities in the low to mid density range ($0.1 \text{ g/cm}^3 \leq \rho \leq 0.3 \text{ g/cm}^3$). Note that in polar and glacier regions, snow may be found with

densities reaching $\rho \approx 0.85 \text{ g/cm}^3$ (Mellor 1977), the cut off between snow and ice. At such densities all of the pores are isolated from one another.

The Role of Surface Area in Microstructure Metamorphism

Regardless of the type of microstructure possessed by snow it is a thermodynamically active material. This characteristic is primarily due to the fact that snow has a large relative surface area. Specific surface areas may be as large as $10,000 \text{ m}^2/\text{m}^3$. As a result, snow is always trying to reduce that area, thereby reducing its large free surface energy, and moving it closer to an equilibrium state (e.g. de Quervain 1963; Hobbs 1965). This surface energy and the high homologous temperature ($T/T_m > 0.9$) at which snow is often considered leads to highly mobile water molecules. It is relatively easy for these to evaporate off of a grain's surface, travel through the pore space in vapor form, move along the surface due to surface diffusion, or migrate through the ice's molecular lattice (Hobbs 1965). These migratory molecules are redistributed by moving from high concentrations to regions of lower concentration. There they become bound to the ice surfaces, effectively redistributing some of the ice volume and producing a reduction in the overall surface area. That in turn leads to a reduction in total surface free energy of the system.

This process of surface reduction as the system tries to reach a minimum energy state is played out in several different ways, primarily determined by temperature and the presence or absence of a significant temperature gradient. Overburden pressure can be important (e.g. Maeno and Ebinuma 1983) but is not considered here.

Snow metamorphism processes are often categorized by mechanism and effect. Bond and neck growth are generally attributed to sintering (common in powder metallurgy and ceramics). Grain growth arises due to temperature gradients, in some cases density gradients (Adams and Brown 1990), and grain size variations (Brown et al. 1994). There is an additional process called melt-freeze cycling (not considered here). Temperature gradient phenomena are considered first.

Temperature Gradient Metamorphism

When temperature gradients are imposed over a snow pack (layers of different types of snow, each having its own characteristics) significant changes in grain shape, size, and strength may occur. Normally temperature gradients must be sufficiently large ($(\Delta T)/(\Delta z) > 10 \text{ }^\circ\text{C}/\text{m}$, Adams and Brown 1990) and the pore space must be sufficiently interconnected. Under these conditions, depending upon temperature, grain size, and pore size (Adams and Brown 1990), rounded ("equilibrium form", Colbeck 1983) grains will become increasingly faceted. The degree and rate of this transformation depends upon density, temperature, temperature gradient, grain shape, and pore size (Colbeck 1983). Grains become more faceted at higher temperature gradients, while at low temperature gradients they are more rounded. Higher temperatures generally accelerate both processes. It is currently understood that most of the mass transport proceeds through both the pores by vapor diffusion and through the ice network by a process referred to as "hand to hand" diffusion (Yosida et al 1955, from Colbeck 1993). This process characterizes water vapor transport between coupled sources and sinks.

If the conditions are sustained long enough, grains can reach a form known as "depth hoar" (de Quervain 1963). It is a weakly bonded, highly faceted grain form. It may be found with hexagonally arranged facets and a cupped base.

According to Perla and Ommanney (1985), the influence of strong temperature gradients is highly dependent upon density. Their findings indicate that in low density newly fallen snow ($\rho \sim 0.1 \text{ g/cm}^3$), evolution is towards large, weakly bonded, "depth hoar" crystals, while older snow ($\rho \sim 0.3 \text{ g/cm}^3$) evolves toward smaller faceted grains in the form of prisms, forming a strong structure known as hard depth hoar.

Sintering and Geometry Driven Metamorphism

The initial form of metamorphism normally undergone by freshly fallen snow is called destructive metamorphism (de Quervain 1963). The snow flakes of fresh snow have large surface areas. A reduction of surface area and surface free energy occurs as the flake's branches decompose into individual fragments. These fragments undergo an additional change as the smaller fragments disappear, a result of mass being transferred to larger fragments. As the larger particles continue to grow at the expense of smaller ones, a gradual evolution toward rounded shapes, known as equilibrium forms (Colbeck 1983), occurs. As these grains come into contact they can obtain a net decrease in surface free energy if they adhere to one another (Kingery 1960), due to the removal of twice the area of contact.

The ensuing metamorphism, in the absence of a significant temperature gradient, is a process of bond and neck growth, called sintering (e.g. Kingery 1960; Kuriowa 1961;

Hobbs and Mason 1964; Maeno and Ebinuma 1983). In the absence of external pressures, four mechanisms for transporting mass to the neck regions usually occur: 1) vapor diffusion through evaporation-condensation, 2) surface diffusion through concentration gradients along the neck region and due to surface tension forces, 3) volume diffusion by molecular migration along vacancies in the ice lattice, and 4) viscous and plastic flow of material in the neck regions due to surface tension forces (e.g. Kingery 1960; Kuriowa 1961; Hobbs and Mason 1964; Maeno and Ebinuma 1983). These mechanisms are assumed to be governed by process which conform to equations of the general form

$$\left(\frac{r_b}{r_g}\right)^n = \frac{B(T)}{r_g^m} t,$$

where r_b is the bond radius, r_g is the grain radius, $B(T)$ is a temperature dependent coefficient, t time, and m, n are integers determined by the particular transport mechanism. Early debate on this occurred with regard to the dominant transport mechanism. Kingery (1960) indicated that surface diffusion is a dominant mechanism, while Kuriowa (1961) proposed volume diffusion, and Hobbs and Mason (1964) claimed vapor diffusion was the dominant process. Resolution of this question did not happen until the work of Maeno and Ebinuma (1983). They showed, using pressureless sintering diagrams, that vapor diffusion and surface diffusion were dominant, depending upon the ratio r_b/r_g and T/T_m (grain size and temperature).

There is one other driving mechanism that has been considered by several researchers. It is often referred to as "equi-temperature" metamorphism, which as Colbeck (1980) points out, is a misnomer, and that it should be called something like "grain curvature-metamorphism". As the last name suggests this type of metamorphism is concerned with

how variations in surface curvature affect metamorphism. Surface curvature produces a vapor pressure gradient along the surface. Lower pressures are associated with the concave necked regions (relative to the ice) and higher pressures occur over the convex surfaces (Colbeck 1980, Brown 1994). Findings indicate that when r_b/r_g is small, this effect may dominate, as long as there is no overriding temperature gradient. The relative bond growth equations for the two dominant sintering mechanism, given by Maeno and Ebinuma (1983), demonstrate how curvature effects may dominate the early stages of sintering. The general form of the growth equations given is

$$\frac{\dot{r}_b}{r_g} = \frac{A(T)}{r_g} K_1^n \quad (n=2, \text{ vapor transport; } n=3, \text{ surface diffusion})$$

where

$$K_1 = \left(\frac{2}{r_g} + \frac{1}{r_b} - \frac{1}{r_n} \right) \left(1 - \frac{r_b}{r_g} \right)$$

and $A_n(T)$ is an appropriate temperature dependent coefficient. Curvature effects are produced by the K_1 where $1/r_g$ is the average grain curvature and $1/r_n$ and $1/r_b$ are the two principal neck curvatures (one parallel to the bond, $1/r_b$, and the other perpendicular to that $1/r_n$).

The work of Brown et al. (1994) is important in that both sintering and radius of curvature metamorphism were accounted for. Brown also demonstrated in a numerical simulation the effects of relative grain growth on grain size, deposition rates along the neck, vapor velocities along the neck, as well as the effects on bond growth due to decrease in source-grain size. Though there was an associated experimental study, also using spherical

particles, some of the necessary measurement techniques were not available. The experimental results presented were inadequate to verify the analytical and numerical calculations.

Since their last study, Brown et al. (1996, 1997a,b), developed a mixture theory formulation of ET metamorphism. It models the material as a distribution of particle sizes, simultaneously, where each group of particle sizes are treated as a separate phase. An accompanying numerical simulation was presented which examined a system with five distinct grain sizes (initial condition). Two different distributions of these 5 particle sizes were evaluated, one based upon initially equal numbers and the other based upon initially equal volume fractions. In both cases, as consequence of the growth of larger particles, there was a reduction in the number of small particles. The rate at which particle size-distributions changed and the manner in which those changes occurred, were shown to be dependent upon the initial material microstructure.

Unfortunately, virtually no experimental data which documents changes in microstructure during metamorphism exists. Other than the partial results presented in Brown et al. (1994) and the measurement of bond radius for individual pairs of equal size spherical ice grains (Kingery 1963), no relevant experimental studies, providing measurements of microstructure parameters as they change over time and at different temperatures, are available. Though the theoretical and numerical results give results qualitatively similar to a few experimental investigations of natural snow involving microstructure measurements (e.g. Keeler 1969; Kry 1975a,b; Gubler 1978a,b; Good 1975, 1989; Good and Krusi 1992), it is essential that an experimental study be conducted with grains corresponding to

those assumed in the theory. Only in that way can the physics of the theory be validated without concern for such things as the effects of grain shape.

1.3 Measurement of Snow Microstructure

Historically, the tools and technology available for measuring snow microstructure have been inadequate, so much so that even the ability to characterize microstructure has been adversely affected. In this section a brief discussion of microstructure measurement is presented.

Two of the most common methods by which microstructure is observed are thin sections, which are thin partially transparent slices (thickness $<30\ \mu\text{m}$, Good 1975) and surface sections, which are opaque plane cross sections (Kry 1975a; Perla 1982; Perla et al. 1988). Thin sections tend to be both difficult to make and time consuming (Kry 1975a). Because they are not single planes, their analysis using Stereology (Chapter 2) presents additional difficulties not encountered with true plane sections. They do have the advantage that (Perla 1985; Dozier et al. 1987) grain boundaries may be visible when sections are viewed with polarized light. For geometric characterization, plane sections offer simpler preparation techniques, faster preparation, and more straight forward analysis when using stereology. However, surface sections also present problems. Sample preparation is also labor intensive, and often grain/pore interfaces are not clearly defined. These interfaces also tend to migrate due to ice sublimation when the surface section is exposed to the air. One of the biggest obstacles to overcome in microstructure measurement, when using

stereology, is characterizing microstructure in such a way that it is amenable to measurement, via stereology. Referring back to the last section, we see that the preferred geometric parameters include mean values for the size of such things as grains, bonds, necks, and pores. Number densities, for example number of bonds per volume, are also important.

Kry (1975a) appears to be the first snow researcher to really exploit the potential of stereology to infer three dimensional parameter values from two dimensional measurements. In that important work he introduced an operational definition of a bond, describing it as it would appear on a surface section. He also showed how an existing stereology relation could be used to relate those bonds on the section plane to a mean 3D bond radius (assumed circular disk shaped bonds) and area. Bonds and grains are really complementary geometric features of an ice network microstructure. By defining bonds as they appear on a section plane, Kry presented a working definition of grain cross sections. With this work, he overcame one of the major hurdles of microstructure parameter evaluation. His methods were then applied to a study of visco-elastic properties and their relation to microstructure (Kry 1975b). A very strong case for the dependence of visco-elastic properties on mean bond radius, bond area, and neck length were made.

A modified form of Kry's bond location criteria was used by Gubler (1978b) in a study to determine the relationship between stereology parameters and tensile strength of snow. An important contribution of this paper was a procedure by which 3D coordination numbers could be obtained from distributions of 2D coordination numbers (number of bonds per grain). A strong correlation between 3D coordination number and strength was found. One problem associated with Gubler's method was an apparent lack of self-constancy. That was remedied by Hansen (1985).

To examine changes in microstructure when snow undergoes large deformations, Edens (1989; Edens and Brown 1991; Brown and Edens 1991) developed a semi-automated software package for snow surface section analysis. It used Kry's (1975a) bond identification criteria (applied visually). An attempt was also made to measure changes in neck length. Coordination numbers were estimated using software developed by Hansen (1985) and was based upon his modifications of Gubler's (1978b) procedure. Though successful in measuring most microstructure parameters of interest, neck length proved to be unsuccessful.

Though it may appear that progress in microstructure characterization and measurement have been adequate, major problems still exist. As stated, the Kry bond criteria has an unfortunate ambiguity, namely what is meant by grain size. Gubler's criteria is no better since it uses the term "obvious" as a major quantifier. Even more troubling is that, ambiguities aside, both methods are difficult to apply objectively and consistently, since previous procedures have not afforded a non-visual inspection-based approach to criteria application (Dozier et al. 1987). Dozier et al. (1987) were reserving judgment on the usefulness of the Kry-Gubler bond criteria, pending improvements in technology. Edens (1989) also found the lack of objectivity and consistency associated with visual-inspection to be problematical. They were implicated as being a major contributor to the unsuccessful attempts to measure changes in neck length.

The above discussion describes the current state-of-the-art in the use of stereology to measure microstructure. Progress in stereology and mathematical morphology as applied to materials science has continued (e.g a nice review by Liu 1993). But the type of devel-

opments needed to remedy the bond-neck objectivity problem do not appear to have been solved as far as the author has been able to determine.

1.4 The Current State of Snow Mechanics and Snow Physics

At the 1995 workshop on "Future Directions in Snow and Ice Research", attendees of the snow portion (many of the top snow researchers in the world) generally agreed, as outlined in the final report (Brown and Dent 1995) that future progress in snow mechanics and snow physics hinges upon an ability to measure microstructure and to relate microstructure to macroscopic processes and behavior. With that and the presentation of the previous sections, it is time to describe the purpose of this thesis.

1.5 Purpose of this Work

Most of the previous microstructural analyses have been conducted for the purpose of relating mechanical loading properties and deformation to microstructure. Similar studies for snow metamorphism are sorely lacking. It ought to be apparent that even if relevant experiments were run, problems in measurement would still need to be overcome.

With the critical need for data regarding microstructure and metamorphism, particularly for compacts of spherical particles (see end of section 1.3) the purpose of this thesis can be stated as follows:

1) Develop a procedure which will allow objective and consistent identification of sectioned bonds and necks,

2) to show that well defined criteria can be stated, thereby removing the ambiguities present in the Kry-Gubler (Kry 1975a; Gubler 1978b) criteria, as well as the criteria used by Edens (1989) to identify sectioned necks,

3) provide crucial data on microstructure evolution of spherical ice particle compacts ("model snows") due to microstructure metamorphism.

Chapter 2 provides an overview of pertinent procedures, terminology, and relationships of stereology. The foundation of objectives 1 and 2 above is called skeletonization. Definitions and algorithms are presented in Chapter 3. Chapter 4 is devoted to development of bond and neck identification criteria. Results and analysis of the experimental study in objective 3 are presented in Chapter 5. A conclusion and suggestions for further research conclude this thesis (Chapter 6).

CHAPTER 2

STEREOLOGY

In Chapter 5, snow microstructure evolution is examined. Measurements will be needed in order to evaluate 3-D microstructural parameters, which characterize the materials current microstructural state. Observations and measurements will be limited to those obtainable from plane sections cut through the microstructure. From section planes it is possible to obtain, counts, lengths, and area measurements. Immediately we see that some disparity exists between what can be measured and what we wish to measure. Fortunately, this doesn't necessarily preclude one from inferring useful information about 3-D microstructure from lower dimensional measurements.

Stereology methods provide the mathematical tools necessary for going from zero (counts), one (lengths), or two (area) dimensional measurements of a microstructure, to associated 3-D parameters of the microstructure itself. Statistical methods are required since the method in which measurements are made is in essence the same as sampling the microstructure under study. The theoretical relationships between sample geometries and the structural geometry follow from Geometric Probability (Kendall and Moran 1963) and Integral Geometry (Santaló 1976).

The purpose of this chapter is to outline those aspects of stereology that will be needed in the remainder of this thesis. Derivations of specific relations will not be given here.

Detailed discussions of stereology can be found in excellent texts by Dehoff and Rhines (1968), Underwood (1970), and Weibel (1980), among others.

The organization of this chapter is as follows. Terminology, concepts, and basic measurements are examined in section 2.1. Those fundamental stereology formulae which will be used later are presented in section 2.2. Particle volume measurement follows in section 2.3. In section 2.4 stereology of circular disks is presented. Finally, in section 2.5 edge effects and other measurement details are considered.

2.1 Terminology, Concepts, and Basic Measurement

Basic Statistical Relationships

This section gathers together those statistical relations which will be used throughout this thesis (see e.g. Mandel 1984).

Associated with a random variable is a probability distribution or frequency distribution. A random variable is a variable that is subject to chance or random fluctuations. The sequence of possible numerical outcomes assumed by a discrete random variable x during an experiment are denoted by x_1, x_2, x_3, \dots . Associated with each possible outcome x_i is a probability value p_i . This association is determined by the probability distribution.

Because there may be many outcomes associated with an experiment, a way is needed to quantify those outcomes in terms of single typical value. The average is commonly used for this. A mathematically more precise term is the *Expected Value* (mean). The expected value associated with the discrete random variable x is expressed by:

$$E(x) = \sum_i x_i p_i.$$

This is also known as the first moment of the random variable x . The k th moment of the random variable x is given by:

$$E(x^k) = \sum_i x_i^k p_i$$

It is also useful to know the dispersion of outcomes about the expected value. This is normally measured with the variance. It is given by

$$Var(x) = \sum_i (x_i - E(x))^2 p_i.$$

This may also be expressed in terms of its square root, also known as the standard deviation, $\sigma(x) = \sqrt{Var(x)}$. A measure of dispersion relative to the expected value is called the coefficient of variation, $CV(x)$, and is given by:

$$CV(x) = \sigma(x)/E(x)$$

Because an experimenter can not usually make as many measurements as there are possible outcomes to an experiment, a subset (sample) of all the possible outcomes (population) is actually obtained. With the subset of values actually measured, it is desired to estimate both the expectation value and standard deviation associated with a population. If a random sample, x_1, x_2, \dots, x_n , of size n is taken from some population, estimates of the population mean and standard deviation are:

$$estimate(E(x)) = \bar{x} = \frac{1}{n} \sum_{i=1}^n x_i, \quad (1)$$

and

$$\text{estimate}(\sigma(x)) = S(x) = \sqrt{\frac{1}{(n-1)} \sum_{i=1}^n (x_i - \bar{x})^2}. \quad (2)$$

\bar{x} is the sample average and $S(x)$ is the sample standard deviation. The reason for the divisor of $S(x)$ being $n-1$ rather than n is that there are only $n-1$ independent quantities in the equation.

Later we will have use for another type of average called the weighted average. Given a set of weights $\{w_1, w_2, \dots, w_n\}$ corresponding to a sample x_1, x_2, \dots, x_n , the weighted average is given by:

$$\bar{x}_w = \left(\sum_{i=1}^n w_i x_i \right) / \sum_{i=1}^n w_i. \quad (3)$$

The subscript indicates that the average is of the weighted variety. Note that equation (1) is recovered upon letting $w_i = 1$. The k th moment is given by:

$$\widehat{x}_w^k = \left(\sum_{i=1}^n w_i x_i^k \right) / \sum_{i=1}^n w_i. \quad (4)$$

The sample standard deviation for the weighted average is given by (see e.g. Mandel 1984)

$$\sigma_w(x) = \sqrt{\sum_{i=1}^n (x_i - \bar{x}_w)^2 w_i} / \sqrt{\sum_{i=1}^n w_i}. \quad (5)$$

There are two measures of error that are also needed later. The first is called the standard error of the mean. Let x_1, x_2, \dots, x_n , be a random sample of size n from some population with variance $v(x)$. It can be shown that (e.g. Mandel 1984) the variance of the sample average is related to the population variance by:

$$\text{Var}(\bar{x}) = \frac{\text{Var}(x)}{n}.$$

The relation is exact. The standard error of the sample average is the square root of this,

$$SE(\bar{x}) = \sigma(x)/\sqrt{n}. \quad (6)$$

Finally, if the standard error is divided by the sample average \bar{x} , the coefficient of error

$$CE(\bar{x}) = SE(x)/\bar{x} \quad (7)$$

is obtained. It is just the relative standard error of the sample average.

Microstructure and Phases

In this thesis, structure (internal or micro), refers to a specific spatial arrangement of particles (ice-grains) which comprise consolidated snow. The collection of these particles will be referred to as the *grain phase* g . These interconnected ice grains produce a continuous network of ice. This ice network or ice matrix, will be referred to as the *ice phase* i . Associated with an ice matrix is a complementary porous microstructure, called the pore phase. This is the portion of a volume of consolidated snow, not comprised of ice. It is occupied by one or more fluids, usually air and/or water. The pore phase will be designated by π . The space containing the specimen under study, the reference space, will be denoted by X .

The spatial arrangement of grains observed in consolidated snow arise when initially discrete particles are brought into contact. At points (or areas) of contact between these grains, a thermodynamic process called sintering occurs. The result of this process is that between each pair of particles in contact a solid connection is formed. The collection of

these connections are referred to as the bond phase, b . An additional phase designator, called the neck phase, η , will also find use. Details are presented in Chapter 4.

When referring to an arbitrary individual component of a particular phase, that phase designator will be subscripted by i . Again, the primary phase designators are, 1) g for the grain phase, 2) ι for the ice phase, 3) π for the pore phase, 4) b for the bond phase, and 5) η for the neck phase.

Microstructure observations are made with "probes". These probes are zero, one, or two dimensional geometric objects. That is, points, lines, or planes. It is common practice to arrange a number of probe elements into an array or grid. This arrangement is referred to as a *test system*. At the outset it is assumed that test a system's size and shape are known. To make a measurement, we can imagine placing a test system within a reference space X which contains a phase Φ of interest. A part of the test system may lay within Φ . The set of geometric objects formed by this intersection, between the test system and phase Φ , will be referred to as either *profiles* or *traces*. Individual profiles fall into one of three categories, point, lineal, or area and depend upon probe and object geometries.

When measurements in X are made with a point probe (set of P points), that probe will be denoted by $P(X)$, or, when there is no problem with ambiguity, by P . For a system of test lines in X (set of lines having a total length L) that probe will be designated as either $L(X)$ or L . Similarly, systems of test planes in X are denoted by either $A(X)$ or A (total area of planes in X is A).

Elements of a point grid which intersect a phase Φ will be denoted by P_Φ . Profiles from this intersection are points.

When the boundary (surface in three dimensions, plane curve in two dimensions) of Φ is intersected by a test line, a point profile is generated. The set of such intersection will be denoted by $I(\Phi)$ (using Weibel's notation, 1980). A lineal profile is generated by a test line when it intersects either an area in two dimensions or a volume in three dimensions. The total length of such profiles, for a phase Φ , is $L(\Phi)$. $N(\Phi)$ is the number of individual profiles having the same dimension as the probe that generated them (not for point probes though). In this case it is the number of lineal profiles generated by a line probe.

Planar probes can generate three profile geometries. Points, $I(\Phi)$, result when a plane intersects any lineal structure. A plane probe intersecting a surface or interface produces lineal traces, $B(\Phi)$. In the case of a planar probe intersecting a volume Φ , an area profile $A(\Phi)$ (cross section area of volume Φ) results. As with line probes and lineal profiles, $N(\Phi)$ is, in conjunction with planar probes, the number of area profiles.

These profile measurements are usually combined with a measure of the test system's size to give a density (not to be confused with a mass density). This is a natural representation since many of the features of interest are dispersed throughout a material's microstructure and therefore have a natural size measure represented by a density. The notation and form of these densities are defined below and are followed by some examples to help explain them.

For a point probe measure, the point fraction,

$$P_P(\Phi) = \frac{P(\Phi)}{P(X)}$$

is used. It is just the ratio of the number of test points intersecting phase Φ and the total number of test points.

Three line probe densities are in common use. The number of point profiles of a boundary Φ per unit length of test line, is

$$I_L(\Phi) = \frac{I(\Phi)}{L(X)},$$

the length fraction of test line L intersecting phase Φ , is

$$L_L(\Phi) = \frac{L(\Phi)}{L(X)},$$

and the number of lineal phase Φ profiles per unit length of test line, is

$$N_L(\Phi) = \frac{N(\Phi)}{L(X)}.$$

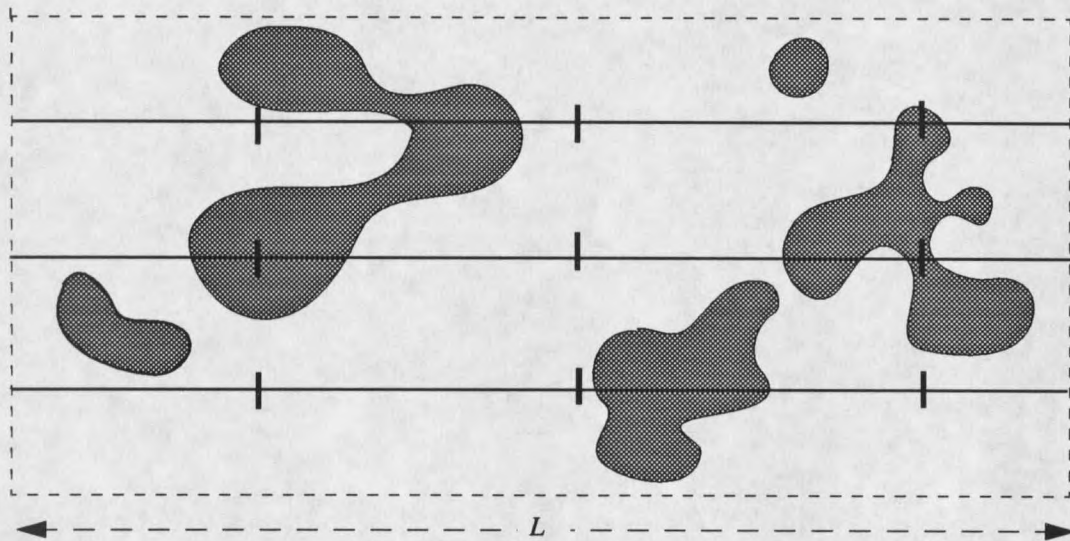


Figure 1. An example of probe measurements. 9 test points in the reference space (intersections of vertical and horizontal lines) intersect the gray-phase 3 times to give a point fraction $P_p(\text{gray}) = 3/9$. Three test lines, each of length L , intercept the gray-phase boundary, black curves, 12 times to give $I_L(\text{black}) = 12/3L$ for the number of point profiles per unit length of test line. There are 6 grey-phase linear profiles from the three line probes, giving $N_L(\text{gray}) = 6/3L = 2/L$ as the number of linear profiles per unit probe length. Within the dashed area A there are 5 grey-phase area profiles, which gives $N_A(\text{gray}) = 5/A$ for the number or area profiles per unit area.

There are two area densities that we will need. They are the number of area profiles per unit probe area

$$N_A(\Phi) = \frac{N(\Phi)}{A(X)},$$

and the area fraction

$$A_A(\Phi) = \frac{A(\Phi)}{A(X)}.$$

It should be noted that several other area densities are possible and that only those of immediate use have been presented.

Image Sampling

Specimen sampling is always accomplished via plane sections. Often measurements are made within sub-regions (quadrats) (Miles 1972) of a section plane. Generally, probes must have orientations which are isotropic with respect to the microstructure, if one is to avoid introducing any orientation bias. That is, orientation invariant measurements are required. To avoid bias due to probe positioning, a test system's origin should be placed according to a uniform-random distribution. The result is translation invariant measurements. Uniform-random imposes spatial homogeneity between probe and specimen. There are a number of ways of guaranteeing that sampling probes satisfy these requirements (see e.g. Miles and Davy 1975; Miles 1978; Gunderson 1981). If the microstructure under study is sufficiently isotropic and homogenous, probe application can be simplified considerably (Miles and Davy 1975; Miles 1978; Karlsson and Cruz-Orive 1991). All that is required is arbitrary placement of sampling probes, i.e. without reference to the micro-

structure. Snow, especially when a specimen has been subjected to little or no temperature gradient or deformation, exhibits a high degree of isotropy and homogeneity (Kry 1975a). For the purposes of this thesis, isotropy and homogeneity will be assumed, whenever stereology measurements are considered.

These assumptions do not eliminate bias (systematic errors) completely. Ratio estimates, in which the denominator is a random variable, exhibit some statistical bias (Cochran 1977). In practice this is usually small and can be ignored. As done by Karlsson and Cruz-Orive (1991), "unbiased" will mean "unbiased for all practical purposes".

2.2 Stereology Formulae

In this section we are interested in the parameters V_V , the volume fraction, S_V , the surface area to volume ratio, and L_3 , the mean 3-D intercept length. These are very general parameters, since no assumptions about object shape are needed.

Volume Fraction V_V

Given a specimen X of volume $V(X)$, composed of several phases, one can specify the fraction of $V(X)$ occupied by any phase Φ_i , by its volume fraction, $V_V(\Phi_i)$. This fraction is given by

$$V_V(\Phi_i) = \frac{V(\Phi_i)}{V(X)}.$$

Any set of phases in X satisfy $\sum V_V(\Phi_i) \leq 1$. Equality holds when the material is saturated (Underwood 1970).

Estimates of volume fraction can be made using any of the three fraction probes discussed in the last section. A simple relation exists between these probe measurements and volume fraction. It is (e.g. Dehoff & Rhines 1968, Underwood 1970, Weibel 1980)

$$V_V(\Phi_i) = A_A(\Phi_i) = L_L(\Phi_i) = P_P(\Phi_i). \quad (8)$$

Volume fraction will be used as a parameter in other stereology formulae and in estimating specimen density. For snow density, it is reasonable to assume that a specimen is composed of two phases, air and ice. If V_S is the volume of a snow specimen, its density ρ_S can be expressed in terms of the volume fractions and densities of air and ice through the relation

$$\rho_S = \rho_a V_V(a) + \rho_i V_V(i).$$

$V_V(a)$ and $V_V(i)$ are the volume fractions of air and ice, respectively. Their corresponding material densities are denoted by ρ_a and ρ_i . Because the density of air is much-much less than that of ice, the contribution of air can be neglected, so that $\rho_S \cong \rho_i V_V(i)$.

Surface Area to Volume Ratio S_V

In a multi phase material, one phase is separated from all others by an inter-phase interface, which for most purposes is just each phase's bounding surface. Discrete objects within a phase are also separated from one another by their individual bounding surfaces.

Knowledge of the density of this surface area is quite important. Its density may be expressed in two ways, surface area of Φ , per unit specimen volume, $V(X)$,

$$S_V(\Phi) = \frac{S(\Phi)}{V(X)},$$

or surface area $S(\Phi)$ of Φ per unit volume $V(\Phi)$ of Φ ,

$$S_{V\Phi}(\Phi) = \frac{S(\Phi)}{V(\Phi)}.$$

In the last expression a reference space other than X was used. The alternate reference space, in this case Φ , was noted in the subscript. This practice will be followed throughout this thesis.

The first of these forms is determined by the stereology relation (e.g. Weibel 1980; Underwood 1970)

$$S_V(\Phi) = 2I_L(\Phi). \quad (9)$$

$I_L(\Phi)$ is the number intercepts of interface Φ per unit length of test line. Notice that for a material with only two phases, Φ_1 and Φ_2 , since they share the same interface, then it follows that $I_L(\Phi_1) = I_L(\Phi_2)$. And, as a result $S_V(\Phi_1) = S_V(\Phi_2)$. The second form of the ratio is given by (Underwood 1970):

$$S_{V\Phi}(\Phi) = \frac{\bar{S}(\Phi)}{\bar{V}(\Phi)} = \frac{S_V(\Phi)}{V_V(\Phi)} = \frac{2I_L(\Phi)}{L_L(\Phi)}. \quad (10)$$

The last equality follows from equations (8) and (9). Equations (9) and (10) are valid for any mixture of surfaces in space, provided all surface intercept directions have equal probability of occurring (Weibel 1980).

In snow science the average coordination number \bar{n}_3 , (mean number of bonds per grain), is an important parameter appearing in both mechanical and thermodynamic models. It is given by:

$$\bar{n}_3 = \frac{2N_V(b)}{N_V(g)}, \quad (11)$$

where $N_V(b)$ is the number of bonds per unit specimen volume, and $N_V(g)$ is the number of grains per unit specimen volume. Without specifying shapes, there is no way of estimating these two densities from a single section plane. Even if one can accurately specify shapes, there are still problems. The main one is a consequence of particle profile counting. Small profiles may not be easily identified, since resolution may not be sufficient to see small features in a section plane. The result may be a significant under-count. Because of the limitations inherent in identifying bonds on a single section, there will almost certainly be an under-count, and not necessarily due to grazing or small profile hits. Less sensitive to these difficulties are corresponding measurements of S_V . This can be used to define a bond density per unit grain surface area, which should exhibit less bias.

We start with equation (11). First, multiply both sides of the equation by the average cross-sectional bond area $\bar{A}(b)$. Then upon dividing by the average surface area per grain $\bar{S}(g)$, the expression

$$\frac{\bar{A}(b)\bar{n}_3}{\bar{S}(g)} = \frac{2N_V(b)\bar{A}(b)}{N_V(g)\bar{S}(g)} \quad (12)$$

is obtained. The total bond surface area per sample volume, $S_V(b)$, is given by the numerator on the right hand side. The denominator is the total grain surface area per sample vol-

ume, $S_V(g)$. It is the sum of the total free ice surface area per sample volume, $S_V(t)$, and $S_V(b)$ i.e. $S_V(g) = S_V(t) + S_V(b)$. Now, substituting into equation (12) gives

$$\frac{\bar{A}(b)\bar{n}_3}{\bar{S}(g)} = \frac{S_V(b)}{S_V(g)} = \frac{S_V(b)}{S_V(t) + S_V(b)} = C_g \quad (13)$$

C_g is called the contiguity (Gurland 1958). It is the average fraction of grain surface area shared with all neighboring grains. The density of bonds per unit grain surface area, N_{3S} , is obtained upon dividing equation (13) by $\bar{A}(b)$;

$$N_{3S} = \frac{C_g}{\bar{A}(b)} \quad (14)$$

It can be written in terms of probe densities by making appropriate substitutions of equation (9) into equation (13). The result is

$$N_{3S} = \frac{2I_L(b)}{2I_L(b) + 2I_L(t)\bar{A}(b)} \cdot \frac{1}{\bar{A}(b)}$$

This is valid for any shape of particle and bond (under the same conditions as S_V in general). Gurland (1958) derived a similar relation under the assumptions of uniform spheres and uniform plates.

Mean Intercept Length L_3

A measure of linear size of a phase Φ is given by the mean intercept length $L_3(\Phi)$. It is given by (Underwood 1970):

$$\bar{L}_3(\Phi) = 2 \frac{L_L(\Phi)}{\bar{I}_L(\Phi)} \quad (15)$$

Because it is inversely proportional to equation (10) it is not a third independent parameter. In some instances it may be a more appropriate size measure than $S_{V\Phi}(\Phi)$. If both the numerator and denominator are measured simultaneously, with the same test system, a simpler form arises:

$$L_3(\Phi) = 2 \frac{L(\Phi)}{\bar{I}(\Phi)}.$$

L_3 measures the average straight line traverse through phase Φ . In the case of a system of uniformly sized spheres, of diameter d , this implies that $L_3 = \frac{2}{3}d$ (Fullman 1953). One additional relation that can sometimes be of use, is obtained by combining equations (10) and (15). When this is done a relationship between the mean intercept length, mean volume, and mean surface area, of phase Φ , is obtained, and is given by

$$L_3(\Phi) = \frac{4\bar{V}(\Phi)}{\bar{S}(\Phi)}.$$

It is occasionally of interest to know the mean free path of particles within the pore space of a material. In a saturated two-phase material of pores (π) and grains (g) ($L_L(g) + L_L(\pi) = 1$), there is a simple relation between mean free path and the mean grain intercept length. Letting λ_π denote the mean free particle path (mean pore intercept length), it is given by (Dehoff and Rhines 1953):

$$\lambda_\pi = 2 \frac{L_L(\pi)}{I_L(\pi)} = 2 \frac{1 - L_L(g)}{I_L(g)} = 4S_V^{-1}(g) - L_3(g). \quad (16)$$

2.3 Volume Weighted Mean Particle Volume \bar{v}_V

An additional measure of particle size, \bar{v}_V , the *volume weighted mean particle volume*, can be estimated from a single surface section. No assumptions regarding specific particle shapes are needed. This is particularly useful when particles have shapes not easily described by standard geometries. In snow studies, where preparing surface sections is extremely time consuming, making serial sections is often impractical. In those cases \bar{v}_V provides the only general expression of particle volume which can be determined from a single surface section. An additional advantage is that the second moment, $\overline{v_V^2}$, can also be estimated from the same surface section.

Volume is an important parameter when examining grain growth, since grain growth implies an addition or subtraction of mass. It is the amount of material that characterizes a grain's size. This is even more important when grains are not spherical, in which case radius may not be the most suitable parameter for characterizing average size. Although, \bar{v}_V is related to the average particle volume \bar{V} , they are not equal unless all particles have the same volume. In measuring average volume, each particle's volume $v(Y_i)$ is weighted in proportion to its volume fraction, where $w_i = v(Y_i)/\sum v(Y_i)$ in equation (3). It follows that \bar{v}_V is given by

$$\bar{v}_V = \sum_i v(Y_i) \frac{v(Y_i)}{\sum_j v(Y_j)}$$

This is the same measurement that would be obtained by sieving, where each sieve class is

